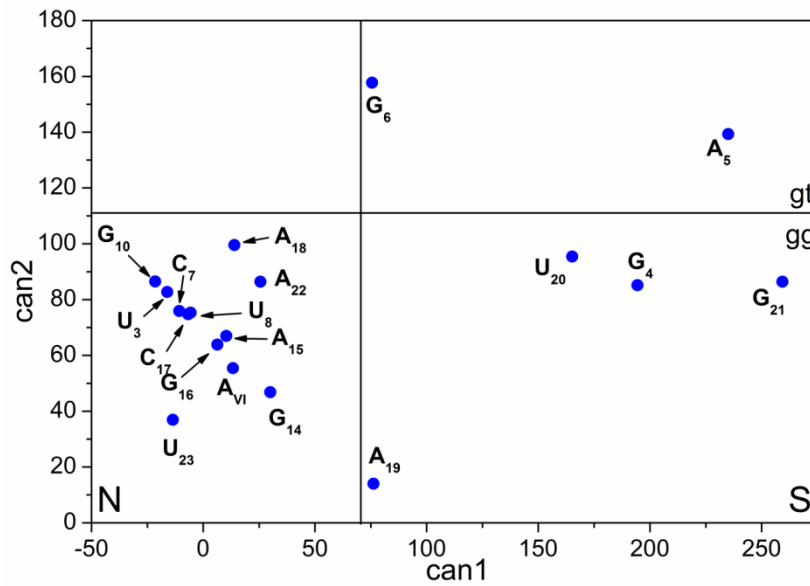


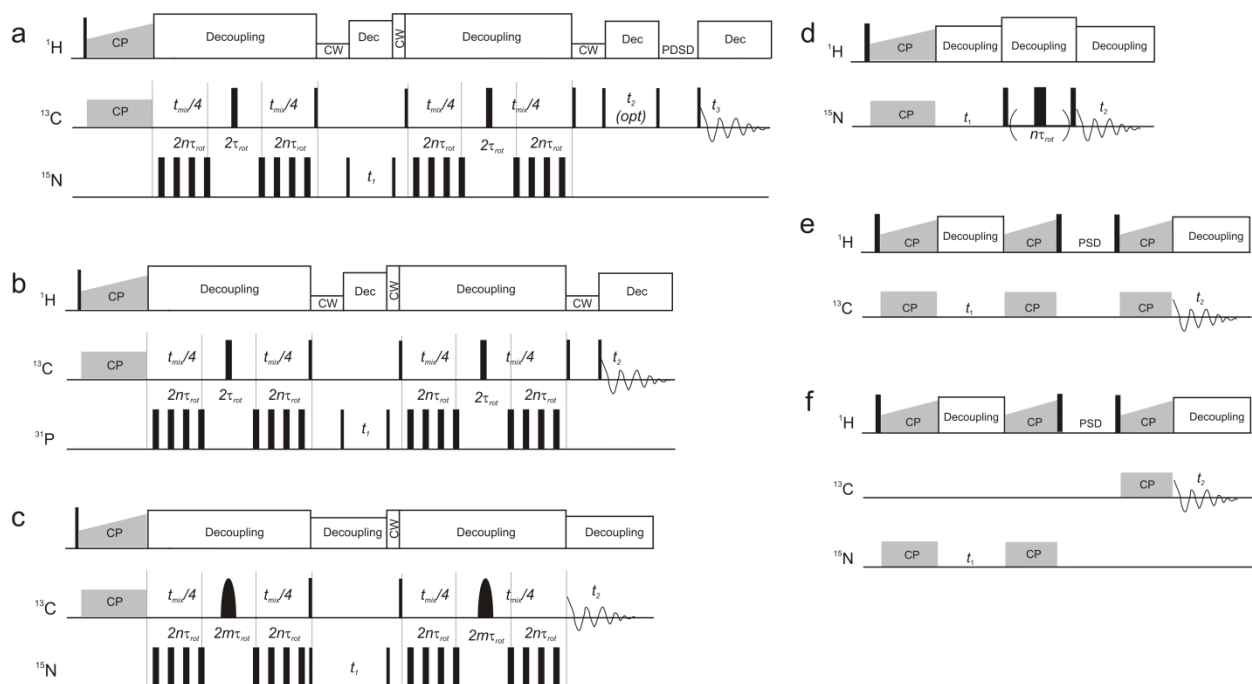
**Supplementary Figure 1 | Overview of samples used for the structure determination of the *Pf* 26mer Box C/D RNA. a, A,C<sup>lab</sup>-RNA, b, A,G<sup>lab</sup>-RNA, c, A,U<sup>lab</sup>-RNA, d, C,U<sup>lab</sup>-RNA, e, G,C<sup>lab</sup>-RNA, f, G,U<sup>lab</sup>-RNA, g, (G-<sup>13</sup>C/A-<sup>15</sup>N)<sup>lab</sup>-RNA, h, (G-<sup>13</sup>C/U-<sup>15</sup>N)<sup>lab</sup>-RNA.**



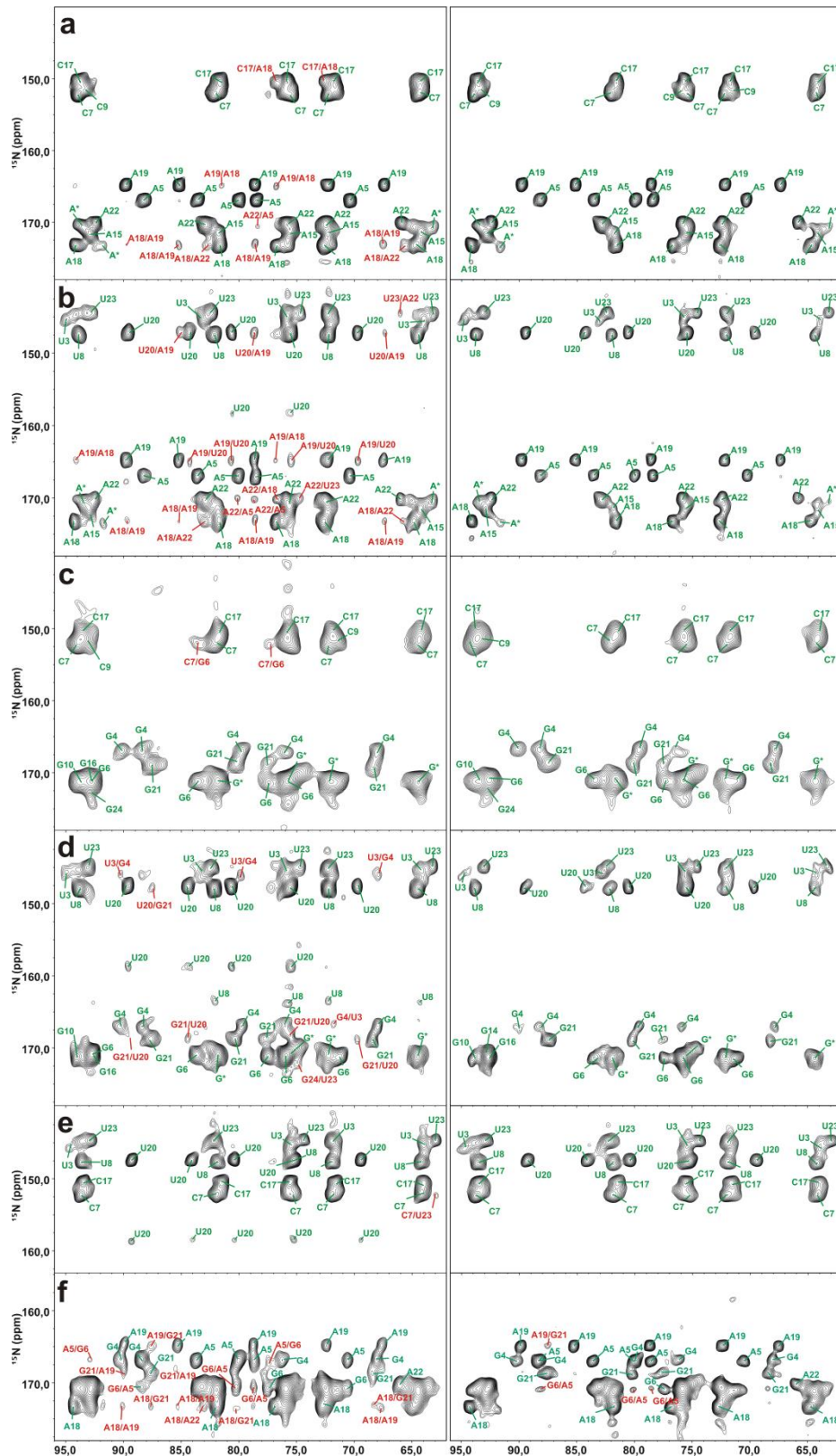
**Supplementary Figure 2 | Canonical coordinates constructed from the ribose chemical shifts.** S (south) and N (north) indicate the C2'-endo and the C3'-endo conformations of the ribose, respectively; gg and gt indicate the gauche/gauche and the gauche/trans conformations of the  $\gamma$  dihedral angle of the RNA backbone<sup>1</sup>.

$$can1 = -14.7\delta_{C1'} + 22.1\delta_{C2'} + 13.3\delta_{C3'} + 6.5\delta_{C4'} - 2.9\delta_{C5'} - 1595$$

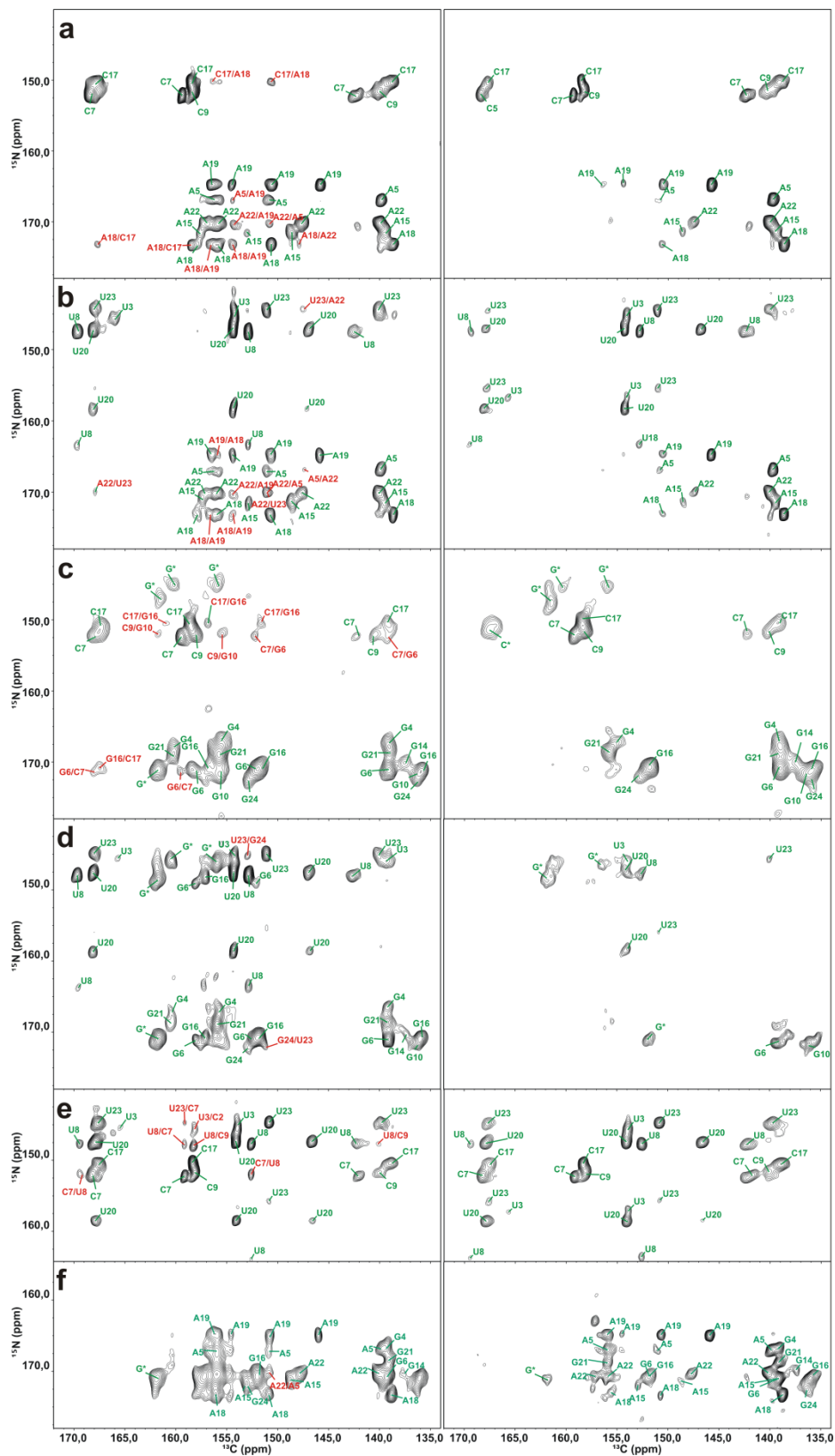
$$can2 = 9.8\delta_{C1'} + 16.5\delta_{C2'} - 0.5\delta_{C3'} - 1.7\delta_{C4'} + 13.5\delta_{C5'} - 2781.$$



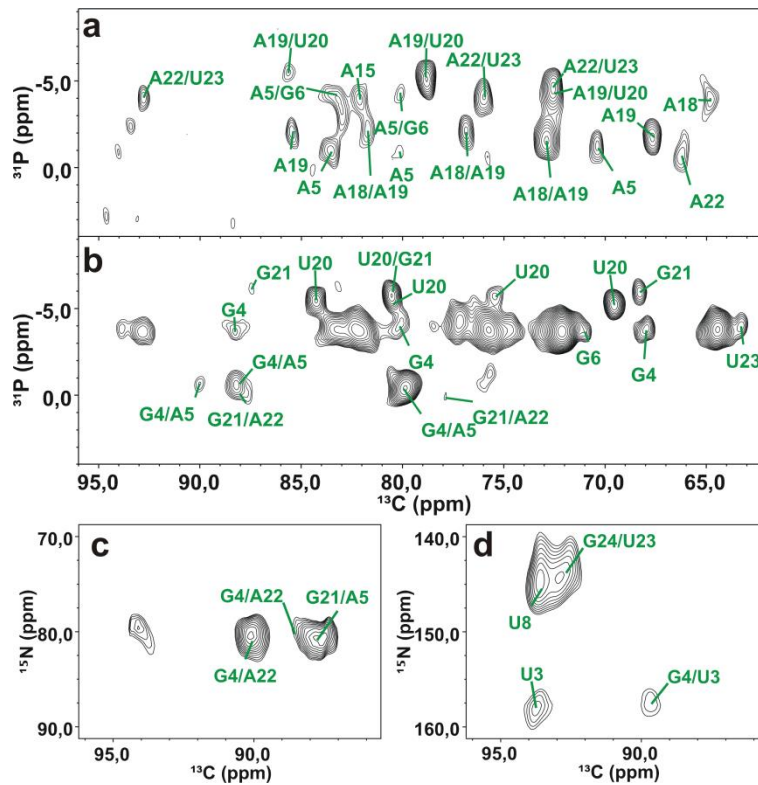
**Supplementary Figure 3 | Pulse sequences for the experiments used in this study.** Narrow and wide solid rectangles represent  $\pi/2$  and  $\pi$  pulses, respectively. In all experiments the  $^1\text{H}$   $\pi/2$  pulse width was 2.7-3.0  $\mu\text{s}$ , while the  $^{13}\text{C}$  and  $^{15}\text{N}$   $\pi/2$  pulse widths were both 6  $\mu\text{s}$ . **a**,  $^{13}\text{C}$ ,  $^{15}\text{N}$ -TEDOR- $^{13}\text{C}$ ,  $^{13}\text{C}$ -PDSD experiment. The TEDOR mixing time,  $t_{\text{mix}}$ , was 1.5-2 ms, the PDSD mixing time was 200-700 ms. **b**,  $^{13}\text{C}$ ,  $^{31}\text{P}$ -TEDOR<sup>2</sup> experiment. The  $^{31}\text{P}$   $\pi/2$  pulse width was 6  $\mu\text{s}$ ; the sensitivity optimized TEDOR mixing time was 3.2 ms. **c**,  $^{13}\text{C}$ -band-selective,  $^{15}\text{N}$ -TEDOR experiment<sup>2</sup>. The width of the band-selective  $^{13}\text{C}$  refocussing pulse was set to 8.5 rotor periods (531.25  $\mu\text{s}$ ), with the  $^{13}\text{C}$  carrier placed at 90 ppm. **d**,  $^{15}\text{N}$ ,  $^{15}\text{N}$ -RFDR experiment<sup>3</sup>. The RDRF mixing time was 20 ms. **e** and **f**, CHHC and NHHC experiments<sup>4,5</sup>. The PSD (Proton Spin Diffusion) mixing time was 100-200  $\mu\text{s}$ . CP, cross polarization; CW, continuous wave decoupling; Dec, decoupling;  $\tau_{\text{rot}}$ , rotor period.



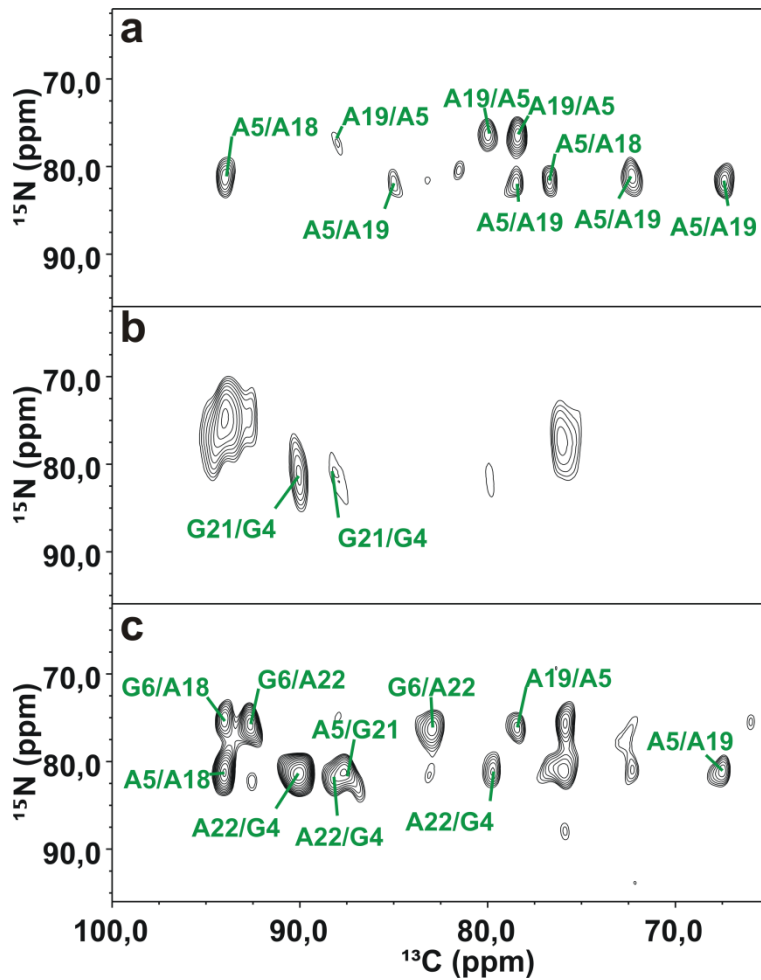
**Supplementary Figure 4 | Ribose regions of 2D  $^{13}\text{C},^{15}\text{N}$ -TEDOR- $^{13}\text{C},^{13}\text{C}$ -PDSB spectra. a, A,C<sup>lab</sup>-RNA, b, A,U<sup>lab</sup>-RNA, c, G,C<sup>lab</sup>-RNA, d, G,U<sup>lab</sup>-RNA, e, C,U<sup>lab</sup>-RNA and f, A,G<sup>lab</sup>-RNA at 700 ms (left) and 100 ms (right) PDSB mixing times. Intra- and inter-nucleotide correlations are indicated in green and red, respectively. Overlapped resonances of guanosines, cytidines and adenosines are labelled as G\*, C\* and A\*. Not assigned resonances in (f) represent overlaps of adenosines and guanosines. The total acquisition time was typically 2 days for 2D spectra at 100 ms mixing time and 4.5 days for 2D spectra at 700 ms mixing time.**



**Supplementary Figure 5 | Base regions of 2D  $^{13}\text{C}$ ,  $^{15}\text{N}$ -TEDOR- $^{13}\text{C}$ ,  $^{13}\text{C}$ -PDS spectra. a,  $\text{A,C}^{\text{lab}}$ -RNA, b,  $\text{A,U}^{\text{lab}}$ -RNA, c,  $\text{G,C}^{\text{lab}}$ -RNA, d,  $\text{G,U}^{\text{lab}}$ -RNA, e,  $\text{C,U}^{\text{lab}}$ -RNA and f,  $\text{A,G}^{\text{lab}}$ -RNA at 700 ms (left) and 100 ms (right) PDS mixing times. Intra- and inter-nucleotide correlations are indicated in green and red, respectively. Overlapped resonances of guanosines, cytidines and adenosines are labelled as G\*, C\* and A\*. Not assigned resonances in (f) represent overlaps of adenosines and guanosines.**

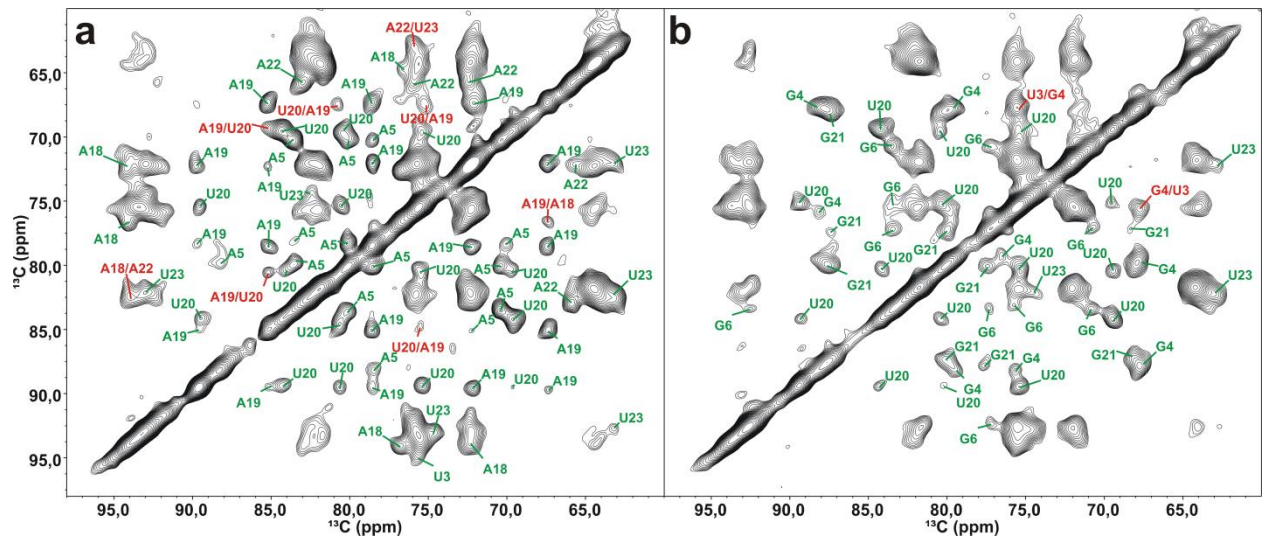


**Supplementary Figure 6 | 2D TEDOR spectra. a-b,**  $^{13}\text{C}$ ,  $^{31}\text{P}$ -TEDOR spectra. **a,**  $\text{A}^{\text{lab}}$ -RNA and **b,**  $\text{G,U}^{\text{lab}}$ -RNA; TEDOR mixing time, 3.2 ms. Non assigned resonances correspond to overlapped nucleotides in helical regions of the RNA. Total acquisition time was 4 days per spectrum. **c-d,**  $^{13}\text{C}$ -band-selective,  $^{15}\text{N}$ -TEDOR spectra. **c,**  $(\text{G-}^{13}\text{C}/\text{A-}^{15}\text{N})^{\text{lab}}$ -RNA and **d,**  $(\text{G-}^{13}\text{C}/\text{U-}^{15}\text{N})^{\text{lab}}$ -RNA (mixing time, 12 ms). The total acquisition time was 5 days per spectrum.



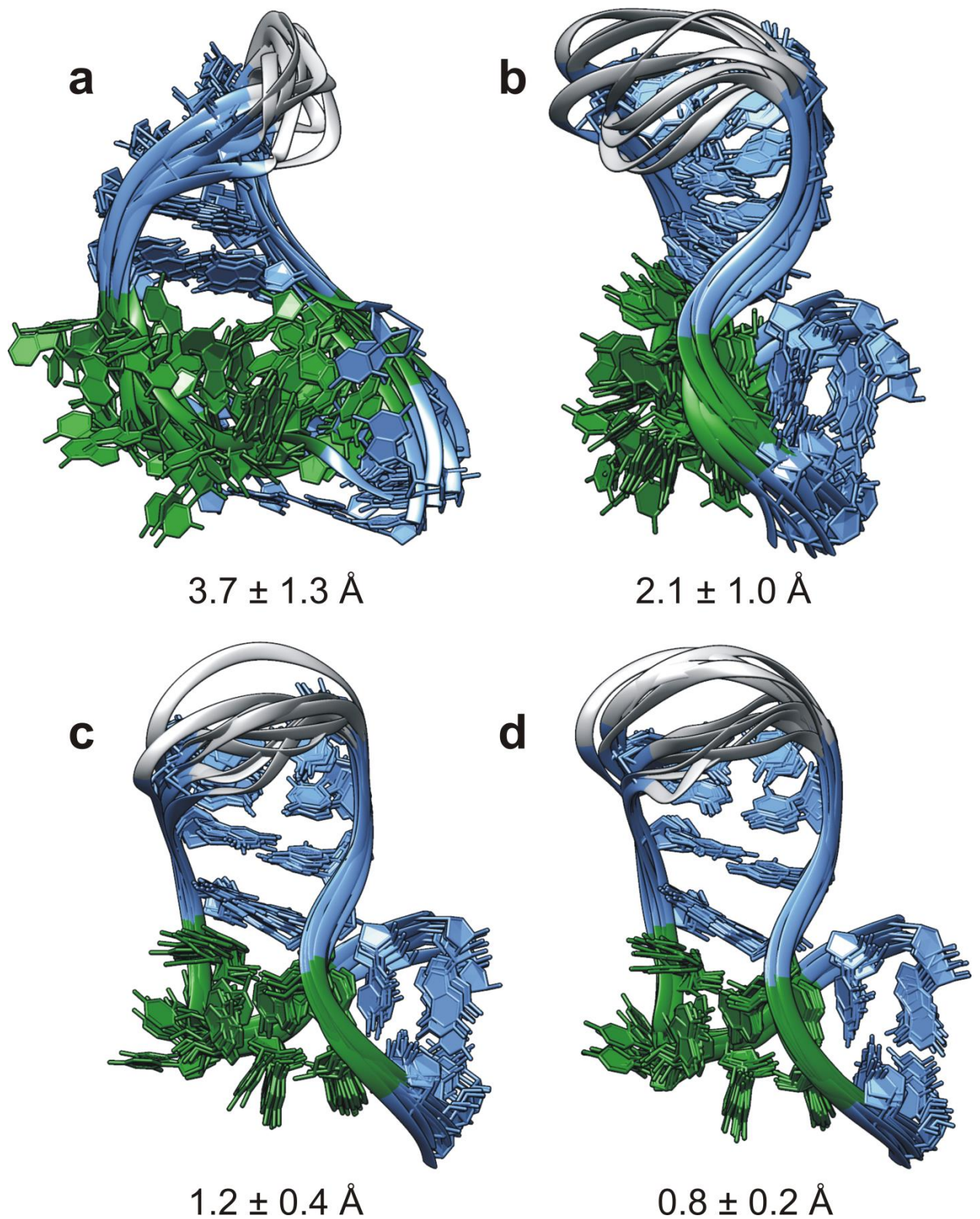
**Supplementary Figure 7 | NHC spectra with 200  $\mu\text{s}$  mixing time. a, A,C<sup>lab</sup>-RNA, b, G,U<sup>lab</sup>-RNA and c, A,G<sup>lab</sup>-RNA. Total acquisition time was 2 days per spectrum for (a) and (c) and 4 days for (b). Not assigned resonances represent non-resolved overlaps. The resolution of the  $^{15}\text{N}$  dimension for the spectrum in (b) was 2.4 times worse than in (a,c).**



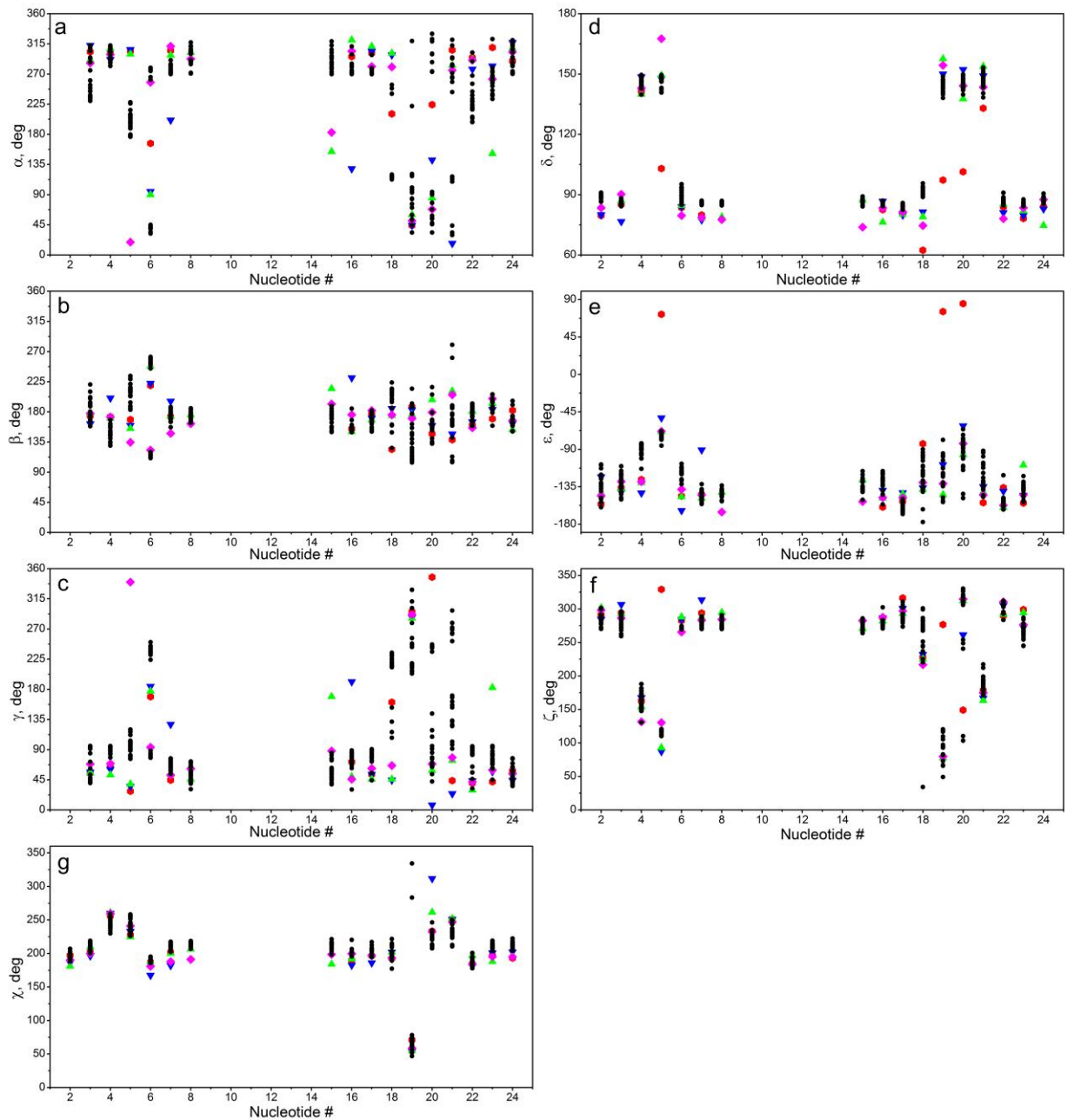


**Supplementary Figure 8 | Ribose regions of CHHC spectra with 200  $\mu$ s mixing time. a, A,U<sup>lab</sup>-RNA, and b, G,U<sup>lab</sup>-RNA. Intra- and inter-nucleotide correlations are indicated in green and red, respectively. Non-assigned resonances correspond to overlapped peaks. The total acquisition time was 2 days per spectrum.**





**Supplementary Figure 9 | Impact of different restraint classes on the precision of the ssNMR structure.** **a**, Dihedral angles restraints and base-pairs restraints only; **b**, as in (a) with the addition of restraints derived from the  $^{13}\text{C}, ^{15}\text{N}$ -TEDOR- $^{13}\text{C}, ^{13}\text{C}$ -PDSO spectra; **c**, as in (b) with the addition of restraints derived from the CHHC and NHHC spectra; **d**, all restraints. Terminal nucleotides 1 and 25-26 are not shown. Helical regions, light blue; k-turn, green; loop, gray. The precision of the first 20 structures is indicated in each panel as the average backbone r.m.s.d. to the mean structure for residues 2-9 and 14-24, excluding the disordered loop and terminal nucleotides.



**Supplementary Figure 10 | Comparison of ribose dihedrals angles for the 20 lowest energy ssNMR structures (black dots) and orthologous X-ray structures. 1RLG<sup>6</sup> (red hexagons), 3NMU<sup>7</sup> (blue triangles), 4BW0<sup>8</sup> (green triangles), 3PLA<sup>9</sup> (magenta diamonds). a,  $\alpha$ ; b,  $\beta$ ; c,  $\gamma$ ; d,  $\delta$ ; e,  $\epsilon$ ; f,  $\zeta$ ; g,  $\chi$ .**

**Supplementary Table 1 | Isotropic chemical shifts of the *Pf* 26mer Box C/D RNA in the L7Ae-Box C/D RNA complex.**

	Isotropic chemical shifts, ppm																	
	C1'	C2'	C3'	C4'	C5'	C2	C4	C5	C6	C8	N1	N2	N3	N4	N6	N7	N9	P
<b>C2</b>	-	-	-	-	-	158.1	-	-	-		-		-	-				-
<b>U3</b>	94.8	75.6	71.9	82.9	64.0	154.1	165.6	104.7	139.3		145.5		157.1					-
<b>G4</b>	90.1	76.0	79.6	88.3	67.8	156.6	155.3	116.7	160.3	139.0	145.0	81.4	-			-	166.9	-3.8
<b>A5</b>	88.1	78.4	80.0	83.4	70.3	<i>156.0</i>	150.9	118.8	<i>156.6</i>	139.8	-		-		81.4	-	166.9	-0.7
<b>G6</b>	92.7	75.8	77.3	83.4	70.9	158.2	152.2	119.5	157.9	139	148.9	75.8	-			-	171.1	-3.8
<b>C7</b>	93.9	75.4	72.1	82.0	64.3	159.3	168.1	97.1	142.2		152.2		196.3	100.0				-
<b>U8</b>	93.7	75.5	72.1	82.1	64.3	152.7	169.4	103.2	142.3		147.7		163.6					-
<b>C9</b>	93.2	75.9	71.4	<i>81.2</i>	64.2	158.2	<i>168.1</i>	98.2	140.2		151.7		197.7	99.1				-
<b>G10</b>	94.0	75.7	71.5	81.8	64.4	-	155.5	-	161.7	136.3	146.2	75.5	-			-	171.3	-
<b>G14</b>	92.6	74.6	-	-	-	155.9	151.9	<i>119.2</i>	-	137.4	147.8	75.4	-			-	170	-
<b>A15</b>	92.9	75.6	72.3	81.8	64.1	<i>153.0</i>	148.6	<i>120.6</i>	<i>157.6</i>	139.5	222.1		-		-	-	171.5	-
<b>G16</b>	92.5	<i>76.0</i>	<i>72.0</i>	81.7	<i>64.4</i>	157.0	151.6	119.0	<i>160.9</i>	135.6	147.6	74.6	-			-	170.9	-
<b>C17</b>	93.6	75.7	71.7	81.6	64.1	158.5	167.6	97.9	139.0		150.5		195.9	99.0				-
<b>A18</b>	94.1	76.6	72.5	81.6	64.6	156.0	150.6	121.6	157.7	138.6	-		-		80.7	230.9	173.2	-4.2
<b>A19</b>	89.7	72.2	78.5	85.1	67.4	154.5	150.5	121.8	156.4	145.8	-		-		76.3	228.2	164.7	-1.8
<b>U20</b>	89.4	75.4	80.5	84.2	69.5	154.2	167.9	105.7	146.8		147.4		158.5					-5.3
<b>G21</b>	87.5	77.5	80.0	87.5	68.3	-	155.7	117.6	160.3	139.0	145.6	81.0	-			-	168.8	-6.0
<b>A22</b>	92.4	75.7	72.4	82.9	65.8	155.9	147.5	121.0	157.1	140.0	-		-		81.2	-	170.2	-0.1
<b>U23</b>	93.0	74.6	72.0	82.3	63.1	151	167.6	103.8	140.0		144.7		155.7					-4.2
<b>G24</b>	92.6	-	-	-	-	<i>157.4</i>	152.8	<i>118.1</i>	-	136.2	-	76.5	-			-	172.4	-

Assignments derived from only one source and/or from overlapped spectral regions are shown in italic.

**Supplementary Table 2 | List of distance restraints used in the structure calculation.**

Atom 1	Atom 2	Atom 2	Atom 2	Restrained distance range (Å)	Distance in the ssNMR structure (Å)
<sup>13</sup> C, <sup>15</sup> N TEDOR- <sup>13</sup> C, <sup>13</sup> C PDS					
C17	C1'	G16	C4	3.5-9.0	5.8
C17	C1'	G16	C6	3.5-9.0	6.7
C17	C1'	G16	C2	3.5-9.0	5.8
C17	C1'	G16	C8	3.5-9.0	6.7
C17	C1'	G16	C1'	3.5-9.0	6.1
C7	C1'	G6	C4'	3.5-9.0	7.2
C7	C1'	G6	C3'	3.5-9.0	5.7
C7	C1'	G6	C5'	3.5-9.0	8
C7	C1'	G6	C1'	3.5-9.0	6.8
C7	C1'	G6	C8	3.5-9.0	7.5
C7	C1'	G6	C4	3.5-9.0	6.4
G6	C1'	C7	C2	3.5-9.0	6.9
G6	C1'	C7	C4	3.5-9.0	6.3
G6	C1'	C7	C5	3.5-9.0	5.6
G16	C1'	C17	C4	3.5-9.0	6.1
C9	C1'	G10	C4	3.5-9.0	6.7
C9	C1'	G10	C6	3.5-9.0	6.4
U20	C1'	A19	C3'	3.5-9.0	6.5
U20	C1'	A19	C2'	3.5-9.0	8.1
U20	C1'	A19	C4'	3.5-9.0	6.4
U20	C1'	A19	C5'	3.5-9.0	6.6
A19	C1'	U20	C2'	3.5-9.0	7.9
A19	C1'	U20	C3'	3.5-9.0	7.1
A19	C1'	U20	C4'	3.5-9.0	6.5
A19	C1'	U20	C5'	3.5-9.0	5.2
A19	C1'	A18	C1'	3.5-9.0	8
A19	C1'	A18	C2'	3.5-9.0	6.8
A18	C1'	A19	C4'	3.5-9.0	6.9
A18	C1'	A19	C3'	3.5-9.0	7.6
A18	C1'	A19	C5'	3.5-9.0	5.4
A18	C1'	A19	C2	3.5-9.0	5.5
A18	C1'	A22	C5'	3.5-9.0	6
A18	C1'	A22	C4'	3.5-9.0	5.7
A18	C1'	A22	C4	3.5-9.0	8.5
A5	C1'	A22	C4	3.5-9.0	5.4
A5	C1'	A22	C5	3.5-9.0	5.7
U23	C1'	A22	C5'	3.5-9.0	7.9
U23	C1'	A22	C4	3.5-9.0	4.8
U23	C1'	A22	C2	3.5-9.0	4.3
U23	C1'	A22	C6	3.5-9.0	5.3
U8	C1'	A15	C4	3.5-9.0	8.6
A22	C1'	U23	C2'	3.5-9.0	7.1
A22	C1'	U23	C4	3.5-9.0	6.4
A22	C1'	U23	C2	3.5-9.0	6.5
A22	C1'	A5	C2'	3.5-9.0	7.9

A22	C1'	A5	C3'	3.5-9.0	8.5
A22	C1'	A18	C2'	3.5-9.0	5.8
A22	C1'	A19	C2	3.5-9.0	7.4
A22	C1'	A5	C4	3.5-9.0	4.9
U3	C1'	G4	C5'	3.5-9.0	5.5
U3	C1'	G4	C3'	3.5-9.0	6.9
U3	C1'	G4	C1'	3.5-9.0	5.6
U20	C1'	G21	C4'	3.5-9.0	6.7
U20	C1'	G21	C5'	3.5-9.0	5.9
G21	C1'	U20	C5'	3.5-9.0	6.2
G21	C1'	U20	C4'	3.5-9.0	6.4
G21	C1'	U20	C1'	3.5-9.0	8.3
G24	C1'	U23	C2'	3.5-9.0	4.8
G24	C1'	U23	C2	3.5-9.0	5.8
U23	C1'	G24	C4	3.5-9.0	5.8
G4	C1'	U3	C3'	3.5-9.0	5
G4	C1'	U3	C4'	3.5-9.0	6.5
G4	C1'	U3	C5'	3.5-9.0	7.4
U8	C1'	C7	C2	3.5-9.0	5.8
U8	C1'	C9	C2	3.5-9.0	5.9
U3	C1'	C2	C2	3.5-9.0	5.8
U23	C1'	C7	C2	3.5-9.0	9.7
C7	C1'	U23	C5'	3.5-9.0	5.7
C9	C1'	U8	C2	3.5-9.0	5.6
C9	C1'	U8	C4	3.5-9.0	6.9
C9	C1'	U8	C5	3.5-9.0	7
U8	C1'	C9	C5	3.5-9.0	4.9
U8	C1'	C9	C6	3.5-9.0	4.7
U8	C1'	C7	C5	3.5-9.0	7.2
C2	C1'	U3	C4	3.5-9.0	5.7
C2	C1'	U3	C2	3.5-9.0	6
C2	C1'	U3	C5	3.5-9.0	5
C17	C1'	A18	C2'	3.5-9.0	6.4
C17	C1'	A18	C3'	3.5-9.0	6.4
C17	C1'	A18	C4	3.5-9.0	6.7
A18	C1'	C17	C2	3.5-9.0	4.2
A18	C1'	C17	C4	3.5-9.0	5.2
C17	C1'	A18	C6	3.5-9.0	8.4
C17	C1'	A18	C2	3.5-9.0	8.3
A19	C1'	G21	C1'	3.5-9.0	5.5
A19	C1'	G21	C3'	3.5-9.0	7.4
G6	C1'	A5	C1'	3.5-9.0	3.9
G6	C1'	A5	C2'	3.5-9.0	5
G6	C1'	A5	C3'	3.5-9.0	5
A5	C1'	G6	C2'	3.5-9.0	5
A18	C1'	G21	C3'	3.5-9.0	8.7
<sup>13</sup> C, <sup>31</sup> P TEDOR					
A19	C4'	U20	P	2.0-5.0	3.7

A5	C3'	A5	P	2.0-5.0	4.5
A5	C3'	G6	P	2.0-5.0	2.6
A5	C4'	G6	P	2.0-5.0	3.3
A22	C1'	U23	P	2.0-5.0	4.8
A5	C4'	A5	P	2.0-5.0	3.8
A19	C4'	A19	P	2.0-5.0	3.8
A18	C4'	A19	P	2.0-5.0	3.7
A18	C2'	A19	P	2.0-5.0	3.8
A22	C2'	U23	P	2.0-5.0	3.5
G4	C1'	A5	P	2.0-5.0	4.5
G4	C4'	A5	P	2.0-5.0	3.4
G4	C4'	G4	P	2.0-5.0	3.9
G4	C3'	G4	P	2.0-5.0	4.9
G21	C4'	G21	P	2.0-5.0	3.9
G21	C4'	A22	P	2.0-5.0	3.6
U20	C3'	U20	P	2.0-5.0	5.2
<sup>13</sup> C, <sup>15</sup> N TEDOR					
G4	C1'	A22	N6	3.0-5.0	3.4
G4	C4'	A22	N6	3.0-5.0	4.5
G21	C1'	A5	N6	3.0-5.0	3.9
G6	C1'	A5	N9	3.0-5.0	4.6
G24	C1'	U23	N1	3.0-7.0	6.1
G4	C1'	U3	N1	3.0-7.0	5.4
CHHC/NHHC					
A18	H2'	A19	H5'	2.0-4.0	3.5
A19	H5'	U20	H3'	2.0-5.0	4.9
A22	H1'	A5	H2	2.0-5.0	3.2
A18	H1'	A22	H4'	2.0-5.0	4.5
A19	H4'	U20	H2'	2.0-5.0	4.4
A19	H4'	U20	H3'	2.0-4.0	3.4
A19	H4'	U20	H5'	2.0-4.0	1.8
A19	H5'	U20	H2'	2.0-5.0	4.7
A22	H2'	U23	H5''	2.0-5.0	4.2
G4	H5'	U3	H2'	2.0-4.0	3.6
G4	H22	G21	H1'	2.0-5.0	5.1
G21	H22	G4	H1'	2.0-5.0	4.8
A19	H62	A5	H2'	2.0-4.0	3.6
A19	H62	A5	H3'	2.0-5.0	5.3
A19	H62	A5	H8	2.0-5.0	4.6
A19	H5''	A5	H61	2.0-4.0	4.9
A19	H4'	A5	H61	2.0-5.0	5.8
A5	H62	A18	H2'	2.0-5.0	6.3
A5	H62	A19	H2'	2.0-5.0	6.2
A5	H61	G21	H1'	2.0-4.0	2.8
A22	H61	G4	H1'	2.0-4.0	2.2
G6	H21	A18	H1'	2.0-4.0	3.8
G6	H22	A22	H4'	2.0-4.0	3.8
G6	H22	A22	H1'	2.0-4.0	4.8

G21	H21	G4	H3'	2.0-5.0	5.8
A22	H61	G4	H3'	2.0-5.0	6
A22	H62	G4	H2'	2.0-5.0	5.1
Intra-nucleotide					
A19	C4'	A19	C8	2.0-6.0	4.7
A19	C4'	A19	C4	2.0-6.0	4.1
A19	C5'	A19	C8	2.0-6.0	5.5
A19	C5'	A19	C4	2.0-6.0	4.3
A19	C5'	A19	C1'	2.0-4.0	3.4
A19	C5'	A19	C2'	2.0-4.0	3.3
A19	H1'	A19	H3'	2.0-5.0	3.8
A19	H1'	A19	H4'	2.0-5.0	3.4
A19	H1'	A19	H5'	2.0-5.0	4.7
A19	H1'	A19	H8	2.0-4.0	2.5
A19	H2'	A19	H4'	2.0-5.0	3.8
A19	H2'	A19	H5'	2.0-5.0	3.1
A19	H3'	A19	H5'	2.0-5.0	2.2
A18	C5'	A18	C4	2.0-6.0	5.3
A18	C4'	A18	C4	2.0-6.0	4.6
A18	C5'	A18	C1'	2.0-4.0	3.5
A18	C5'	A18	C2'	2.0-4.0	3.7
A18	H1'	A18	H3'	2.0-5.0	3.9
A18	H1'	A18	H4'	2.0-5.0	3.6
A18	H2'	A18	H4'	2.0-5.0	3.9
A18	H2'	A18	H5'	2.0-5.0	4.5
A18	H3'	A18	H5'	2.0-5.0	2.3
A18	H4'	A18	H8	2.0-5.0	4.1
A5	C5'	A5	C4	2.0-6.0	5.5
A5	C5'	A5	C1'	2.0-4.0	3.4
A5	C5'	A5	C2'	2.0-4.0	3.3
A5	H1'	A5	H3'	2.0-5.0	3.8
A5	H2'	A5	H4'	2.0-5.0	3.8
A5	H2'	A5	H5'	2.0-5.0	4.3
A5	H2'	A5	H8	2.0-5.0	2.4
A5	H3'	A5	H5'	2.0-5.0	3.5
A22	C5'	A22	C4	2.0-6.0	5.5
A22	C3'	A22	C4	2.0-6.0	4.2
A22	C5'	A22	C1'	2.0-4.0	3.6
A22	C5'	A22	C2'	2.0-4.0	3.7
A22	H4'	A22	H8	2.0-5.0	4.3
A22	H2'	A22	H5'	2.0-5.0	5.4
A22	H3'	A22	H5'	2.0-5.0	3.7
A15	C5'	A15	C1'	2.0-4.0	3.6
A15	C5'	A15	C2'	2.0-4.0	3.7
U3	C5'	U3	C1'	2.0-4.0	3.6
U3	C5'	U3	C2'	2.0-4.0	3.7
U3	C5'	U3	C2	2.0-6.0	5.6
U8	C5'	U8	C1'	2.0-4.0	3.6



U8	C5'	U8	C2'	2.0-4.0	3.7
U8	C5'	U8	C2	2.0-6.0	5.6
U20	C5'	U20	C1'	2.0-4.0	3.3
U20	C5'	U20	C2'	2.0-4.0	3.2
U20	C5'	U20	C2	2.0-6.0	5.4
U20	C5'	U20	C6	2.0-6.0	3.8
U23	C5'	U23	C1'	2.0-4.0	3.6
U23	C5'	U23	C2'	2.0-4.0	3.7
U23	C5'	U23	C2	2.0-6.0	5.6
G4	C5'	G4	C1'	2.0-4.0	3.4
G4	C5'	G4	C2'	2.0-4.0	3.3
G6	C5'	G6	C1'	2.0-4.0	3.5
G6	C5'	G6	C2'	2.0-4.0	3.7
G10	C5'	G10	C1'	2.0-4.0	3.5
G10	C5'	G10	C2'	2.0-4.0	3.7
G21	C5'	G21	C1'	2.0-4.0	3.5
G21	C5'	G21	C2'	2.0-4.0	3.4
C7	C5'	C7	C1'	2.0-4.0	3.6
C7	C5'	C7	C2'	2.0-4.0	3.7
C9	C5'	C9	C1'	2.0-4.0	3.6
C9	C5'	C9	C2'	2.0-4.0	3.7
C17	C5'	C17	C1'	2.0-4.0	3.6
C17	C5'	C17	C2'	2.0-4.0	3.7

---

## Supplementary references

1. Cherepanov, A. V., Glaubitz, C., & Schwalbe, H. High-resolution studies of uniformly C-13,N-15-labeled RNA by solid-state NMR spectroscopy. *Angew. Chem. Int. Ed.* **49**, 4747-4750 (2010).
2. Jaroniec, C. P., Filip, C., & Griffin, R. G. 3D TEDOR NMR experiments for the simultaneous measurement of multiple carbon-nitrogen distances in uniformly C-13, N-15-labeled solids. *J. Am. Chem. Soc.* **124**, 10728-10742 (2002).
3. Bennett, A. E., Ok, J. H., Griffin, R. G., & Vega, S. Chemical-shift correlation spectroscopy in rotating solids - Radio Frequency-driven Dipolar Recoupling and longitudinal exchange. *J. Chem. Phys.* **96**, 8624-8627 (1992).
4. Lange, A., Luca, S., & Baldus, M. Structural constraints from proton-mediated rare-spin correlation spectroscopy in rotating solids. *J. Am. Chem. Soc.* **124**, 9704-9705 (2002).
5. Lange, A., *et al.* A concept for rapid protein-structure determination by solid-state NMR spectroscopy. *Angew. Chem. Int. Ed.* **44**, 2089-2092 (2005).
6. Moore, T., Zhang, Y. M., Fenley, M. O., & Li, H. Molecular basis of box C/D RNA-protein interactions: Cocrystal structure of archaeal L7Ae and a box C/D RNA. *Structure* **12**, 807-818 (2004).
7. Xue, S., *et al.* Structural basis for substrate placement by an archaeal Box C/D ribonucleoprotein particle. *Mol. Cell* **39**, 939-949 (2010).
8. Huang, L. & Lilley, D. M. The molecular recognition of kink-turn structure by the L7Ae class of proteins. *RNA* **19**, 1703-1710 (2013).
9. Lin, J., *et al.* Structural basis for site-specific ribose methylation by box C/D RNA protein complexes. *Nature* **469**, 559-563 (2011).